Theoret. Appl. Mech., Vol.33, No.1, pp. 65–90, Belgrade 2006

Analysis of stress and strain in a rotating disk mounted on a rigid shaft

Nelli N. Alexandrova * **Sergei Alexandrov** †
Paulo M. M. Vila Real ‡

Abstract

The plane state of stress in an elastic-perfectly plastic isotropic rotating annular disk mounted on a rigid shaft is studied. The analysis of stresses, strains and displacements within the disk of constant thickness and density is based on the Mises yield criterion and its associated flow rule. It is observed that the plastic deformation is localized in the vicinity of the inner radius of the disk, and the disk of a sufficiently large outer radius never becomes fully plastic. The semi-analytical method of stress-strain analysis developed is illustrated by some numerical examples.

Keywords: Rotating shaft-disk assembly, plane stress, strain distribution, Mises yield criterion, semi-analytical solution.

*Department of Civil Engineering, University of Aveiro, 3810-193 Aveiro, Portugal, e-mail:nalexandrova@civil.ua.pt

†Institute for Problems in Mechanics, Russian Academy of Sciences, 101-1 Prospect Vernadskogo, 119526 Moscow, Russia, e-mail:sergei_alexandrov@hotmail.com

‡Department of Civil Engineering, University of Aveiro, 3810-193 Aveiro, Portugal, e-mail:pvreal@civil.ua.pt

Notations:

A, B	constants of integration;
a, b	inner and outer radii of the disk, respectively;
c	radius of elastic-plastic boundary;
E	modulus of elasticity;
k	shear yield stress;
q	ratio of inner to outer radius of the disk;
u	non-dimensional radial displacement;
$r\theta$	plane polar coordinate system;
s_r, s_θ	non-dimensional deviator components of the stress tensor;
β	non-dimensional polar radius;
γ	non-dimensional radius of elastic-plastic boundary;
ε	total strain tensor;
$\varepsilon_r, \varepsilon_\theta$	components of the total strain tensor;
$\varepsilon^e, \varepsilon^p$	elastic and plastic portions of the total strain tensor, respectively;
$\varepsilon_r^p, \varepsilon_\theta^p$	plastic components of the strain tensor in the plastic zone;
$\varepsilon_r^e, \varepsilon_\theta^e$	elastic components of the strain tensor in the plastic zone;
$\varepsilon_r^E, \varepsilon_\theta^E$	elastic components of the strain tensor in the elastic zone;
φ	function of r ;
φ_e	value of φ at $\Omega = \Omega_e$ and $\beta = q$
$\varphi_q, \varphi_\gamma$	values of φ at $\beta = q$ and $\beta = \gamma$, respectively;
$\Phi_1, \Phi_2, \Phi_3,$	
Φ_4, Φ_5, Φ_6	functions of φ ;
ν	Poisson's ratio;
ρ	density of the material;
σ_r, σ_θ	non-dimensional components of the stress tensor;
$\xi_r^p, \xi_\theta^p, \xi_r^e, \xi_\theta^e$	derivatives of $\varepsilon_r^p, \varepsilon_\theta^p, \varepsilon_r^e, \varepsilon_\theta^e$ with respect to Ω ;
ω	angular velocity;
ω_e	angular velocity at the initial yielding;
$\Omega, \Omega_e, \Omega_{\max}$	non-dimensional angular velocity parameters.

1 Introduction

An annular disk mounted on a circular shaft rotating at high speed is widely used in engineering applications. Numerous works have been published on analysis and design of such disks. In the case of elastic/plastic disks, the study of stress and strain fields in rotating disks has begun with models based on the Tresca yield criterion. A review of these works is given in [1]. Other piece-wise linear yield criteria have been adopted in [2, 3]. It has been mentioned in [1] that the analysis based on the Tresca yield criterion is simpler than that based on the Mises yield criterion. However, in fact, it depends on loading conditions, and matching different regimes on the Tresca yield surface can require so cumbersome algebraic transformations that the differential formulation following from the Mises constitutive equations looks much simpler [4]. On the other hand, the development of computational models for plane stress elasto-plasticity meets some difficulties which do not exist in 3D and plane strain formulations [5]. Therefore, it seems that an appropriate approach to deal with disk problems under plane stress conditions is to advance the analytical treatment of the system of equations as much as possible and, then, to solve the resulting equation (or equations) numerically. In the case of the Mises yield criterion, such an approach has been developed [4, 6 – 8] for a class of problems for thin plates and disks. In particular, a hollow rotating disk with pressures prescribed at its inner and outer counter has been studied in [4, 8]. In the present paper, this approach is extended to rotating disks mounted on a rigid shaft. The presence of the shaft leads to new qualitative features of the solutions which may be of importance in practical applications and may be helpful in gaining insight into the nature of possible numerical difficulties while solving more complex (geometrically or physically) problems by means of finite element or other similar methods. Note that solutions for thin rotating disks based on the Mises yield criterion are known in the literature, for example [9 - 14]. In all of these studies, a deformation theory of plasticity has been adopted (stresses are related to plastic strains in the plastic zone). Different disk shapes, hardening laws and loading conditions have been investigated, though conceptually all these solutions are very similar to each other.

In contrast, the solution proposed in the present paper, as well as the solutions given in [6, 8], use the theory of plastic flow (stresses are related

to plastic strain rates in the plastic zone). It makes a significant difference with the solutions [9 – 14] in both the formulation of the problem and the result obtained. In particular, because of the nature of deformation theories of plasticity, it has been possible to prescribe a simple boundary condition in terms of stress on the surface of a rigid inclusion (shaft) [11], whereas the present formulation requires a condition in terms of velocity (displacement). Moreover, in [12, 13] the fully plastic disk has been considered, whereas the present solution shows that such a state of the disk is almost impossible and the limit angular velocity is determined by another condition.

2 Statement of the problem and elastic loading

Consider a thin disk of material density ρ, shear yield stress k, Young's modulus E, Poisson's ratio ν, outer radius b, inner radius a mounted on a rigid shaft and rotating at an angular speed ω. The problem geometry suggests the use of a plane polar coordinate system $r\theta$ with its origin at the center of the shaft (Fig. 1). When the angular speed is high enough, the plastic zone develops in the region $a \leq r \leq c$ where c is the radius of elastic-plastic boundary. Obviously, the value of c depends on ω. In contrast to the problem of a rotating hollow disk with prescribed pressures at $r = a$ and $r = b$ [4, 8], the problem under consideration is not statically determined (even for perfectly plastic materials) since the only one stress boundary condition is given at $r = b$ whereas the boundary condition at $r = a$ is given in terms of velocity (or displacement). This significantly complicates the solution. Because of the symmetry, the solution is independent of θ.

Within the elastic zone $c \leq r \leq b$ (or, in non-dimensional form, $\gamma \leq \beta \leq 1$) the Hooke's law holds

$$(E/k)\,\varepsilon_r = \sigma_r^{\cdot} - \nu\sigma_\theta^{\cdot} \quad (E/k)\,\varepsilon_\theta = \sigma_\theta^{\cdot} - \nu\sigma_r \tag{1}$$

together with the compatibility equation

$$\varepsilon_r = d\,(\beta\varepsilon_\theta)/d\beta, \tag{2}$$

which is obtained from the well-known strain-displacement relations

$$\varepsilon_r = du/d\beta, \quad \varepsilon_\theta = u/\beta \tag{3}$$

Here σ_r and σ_θ are the non-dimensional (referred to k) radial and circumferential components of the stress tensor, respectively; ε_r and ε_θ are the radial and circumferential components of the strain tensor, respectively; β is the non-dimensional radius,$\beta = r/b$; and u is the non-dimensional (refereed to b) radial displacement; $\gamma = c/b$ is the non-dimensional radius of the elastic-plastic boundary.

The only non-trivial equation of motion is

$$d\sigma_r/d\beta + (\sigma_r - \sigma_\theta)/\beta = -\Omega\beta, \tag{4}$$

where $\Omega = \rho\omega^2 b^2/k$ is the non-dimensional angular velocity parameter. The outer radius of the disk is stress free. Therefore,

$$\sigma_r = 0 \quad at \quad \beta = 1 \tag{5}$$

Both σ_r and σ_θ are to be continuous across the elastic-plastic boundary:

$$[\sigma_r] = 0, \quad [\sigma_\theta] = 0 \quad at \quad \beta = \gamma \tag{6}$$

where square brackets denote the amount of jump in the quantity enclosed in the brackets. Eq. (5) in the case of elastic solution and Eqs. (5)-(6) in the case of elastic-plastic solution constitute the stress boundary conditions which must be supplemented with the displacement boundary conditions. Since the shaft is rigid,

$$u = 0 \quad at \quad \beta = q \tag{7}$$

where $q = a/b$. The other condition, which is only applicable in the case of elastic-plastic solution, is

$$[u] = 0 \quad at \quad \beta = \gamma \tag{8}$$

Upon combining Eqs. (1) - (4), the radial displacement and stress distributions in the elastic zone take the form

$$u = \frac{A\,(1+\nu)}{\beta} + B\beta - \frac{1-\nu^2}{8}\frac{k}{E}\Omega\beta^3 \tag{9}$$

$$\sigma_r = -\frac{A}{\beta^2} + \frac{B}{1-\nu} - \frac{3+\nu}{8}\Omega\beta^2, \tag{10}$$

$$\sigma_\theta = \frac{A}{\beta^2} + \frac{B}{1-\nu} - \frac{1+3\nu}{8}\Omega\beta^2$$

where A and B are constants to be found from the boundary conditions.

For purely elastic loading occurring at small angular speeds, the boundary conditions (5) and (7) result in

$$A = \Omega q^2 \frac{(1-\nu)}{8}\left[\frac{(1+\nu)\,q^2 - (3+\nu)}{(1-\nu)\,q^2 + (1+\nu)}\right], \tag{11}$$

$$B = (1-\nu)\left(\frac{3+\nu}{8}\Omega + A\right)$$

In the case of plastic loading, the representation for B in the form of Eq. $(11)^2$ is still valid. Substituting it into Eqs. (9) - (10) leads to the displacement, strain and stress distributions in the elastic zone of the elastic/plastic disk

$$\frac{E}{k}u = A\left((1-\nu)\,\beta + \frac{1+\nu}{\beta}\right) + \frac{1-\nu}{8}\beta\Omega\left[3+\nu-\beta^2\,(1+\nu)\right] \tag{12}$$

$$\frac{E}{k}\varepsilon_r^E = A\left(1-\nu-\frac{1+\nu}{\beta^2}\right) + \frac{1-\nu}{8}\Omega\left[3+\nu-3\beta^2\,(1+\nu)\right], \tag{13}$$

$$\frac{E}{k}\varepsilon_\theta^E = A\left(1-\nu+\frac{1+\nu}{\beta^2}\right) + \frac{1-\nu}{8}\Omega\left[3+\nu-\beta^2\,(1+\nu)\right]$$

$$\sigma_r = A\left(1-\frac{1}{\beta^2}\right) + \frac{3+\nu}{8}\Omega\left(1-\beta^2\right),$$

(14)

$$\sigma_\theta = A\left(1+\frac{1}{\beta^2}\right)+\frac{3+\nu}{8}\Omega\left(1-\frac{1+3\nu}{3+\nu}\beta^2\right)$$

3 Plastic loading

Within the plastic zone $q \le \beta \le \gamma$, the stress equations consist of the plane stress Mises yield criterion

$$\sigma_r^2+\sigma_\theta^2-\sigma_r\sigma_\theta = 3 \tag{15}$$

and Eq. (4). Assuming that yielding starts at the inner radius of the disk, $\beta = q$, the value of the non-dimensional angular velocity parameter at which the plastic zone appears in the disk, Ω_e, is obtained by substitution of Eqs. (10)-(11) into Eq. (15)

$$\Omega_e = \frac{4\sqrt{3}\left[q^2(1-\nu)+1+\nu\right]}{(1-q^2)\left(\nu^2-\nu+1\right)^{1/2}\left[q^2(1-\nu)+3+\nu\right]} \tag{16}$$

To satisfy the yield criterion (15), the stresses can be represented in the form

$$\sigma_r = \sqrt{3}\cos\varphi-\sin\varphi, \quad \sigma_\theta = -2\sin\varphi \tag{17}$$

This substitution is very similar to the standard substitution introduced in [15]. The equation for $\varphi(\beta, \Omega)$ is determined upon substitution of Eq. (17) into Eq. (4)

$$\left(\sqrt{3}\sin\varphi+\cos\varphi\right)\frac{\partial\varphi}{\partial\beta}-\left(\sqrt{3}\cos\varphi+\sin\varphi\right)\frac{1}{\beta}-\Omega\beta = 0 \tag{18}$$

Using Eq. (11) it is possible to find from Eq. (10) and Eq. (16) that

$$\sigma_r = \sqrt{3}\Big/\sqrt{\nu^2-\nu+1}, \quad \sigma_\theta = \sqrt{3}\nu\Big/\sqrt{\nu^2-\nu+1}$$

at $\Omega = \Omega_e$ and $\beta = q$. Combining these values of the stresses and Eq. (17) determines φ at $\Omega = \Omega_e$ and $\beta = q$ in the form

$$\varphi_e = -\arcsin\left[\sqrt{3}\nu \Big/ \left(2\sqrt{\nu^2-\nu+1}\right)\right] \tag{19}$$

It is interesting to mention that φ_e depends only on Poisson's ratio. Since the coefficient of the derivative in Eq. (18) vanishes at $\varphi = -\pi/6$, it is a singular point of this equation. It is possible to show that its solution cannot be extended beyond this point. Therefore, the admissible range of φ-value is

$$\varphi_e \leq \varphi < -\pi/6 \tag{20}$$

It is convenient to introduce the following functions of φ

$$\begin{aligned}
&\Phi_1(\varphi) = \sqrt{3}\sin\varphi + \cos\varphi, \quad \Phi_2(\varphi) = \sqrt{3}\sin\varphi - \cos\varphi,\\
&\Phi_3(\varphi) = \sqrt{3}\cos\varphi + \sin\varphi, \quad \Phi_4(\varphi) = \sqrt{3}\cos\varphi - \sin\varphi,\\
&\Phi_5(\varphi) = \nu\sqrt{3}\sin\varphi - (2-\nu)\cos\varphi,\\
&\Phi_6(\varphi) = \nu\sqrt{3}\cos\varphi + (2-\nu)\sin\varphi
\end{aligned} \tag{21}$$

Substituting Eq. (14) and Eq. (17) into the boundary conditions (6) yields

$$\gamma^2 = \frac{32\sqrt{\Omega^2 + 2\Omega\Phi_6(\varphi_\gamma) + \Phi_3(\varphi_\gamma)^2} - 2\Phi_3(\varphi_\gamma) - \Omega(1+\nu)}{\Omega(1-\nu)} \tag{22}$$

$$A = \frac{\gamma^2}{1+\gamma^2}\left\{\frac{\Omega}{8}\left[\gamma^2(1+3\nu) + (3+\nu)\right] - 2\sin\varphi_\gamma\right\} \tag{23}$$

where φ_γ is the value of φ at $\beta = \gamma$.

The total strainε in the plastic zone is decomposed into its elastic and plastic parts as

$$\varepsilon_r = \varepsilon_r^e + \varepsilon_r^p \quad and \quad \varepsilon_\theta = \varepsilon_\theta^e + \varepsilon_\theta^p \tag{24}$$

The elastic part is obtained by substituting Eq. (17) into the Hooke's law (1)

$$(E/k)\,\varepsilon_r^e = \sqrt{3}\cos\varphi - (1-2\nu)\sin\varphi,$$

$$(E/k)\,\varepsilon_\theta^e = -\nu\sqrt{3}\cos\varphi - (2-\nu)\sin\varphi \tag{25}$$

Differentiation of these equations with respect to time, which is denoted by the superimposed dot, gives the elastic portions of the strain rate tensor, $\dot{\varepsilon}_r^e$ and $\dot{\varepsilon}_\theta^e$,

$$\begin{gathered}(E/k)\,\dot{\varepsilon}_r^e = -\dot{\varphi}\left[\sqrt{3}\sin\varphi + (1-2\nu)\cos\varphi\right], \\ (E/k)\,\dot{\varepsilon}_\theta^e = \dot{\varphi}\left[\nu\sqrt{3}\sin\varphi - (2-\nu)\cos\varphi\right]\end{gathered} \tag{26}$$

The plastic portions of the strain rate tensor, $\dot{\varepsilon}_r^p$ and $\dot{\varepsilon}_\theta^p$, obey the associated flow rule. A consequence of this rule is

$$\dot{\varepsilon}_r^p/\dot{\varepsilon}_\theta^p = s_r/s_\theta \tag{27}$$

where the components of the stress deviator tensor, s_r and s_θ, follow from Eq. (17) with the use of plane-stress assumption $\sigma_z = 0$

$$s_r = 2\cos\varphi\Big/\sqrt{3}, \quad s_\theta = -\Big(\sqrt{3}\sin\varphi + \cos\varphi\Big)\Big/\sqrt{3} \tag{28}$$

The incompressibility equation for plastic strains determines the strain rate $\dot{\varepsilon}_z^p$. Substituting Eq. (28) into Eq. (27) yields

$$\dot{\varepsilon}_r^p = -2\dot{\varepsilon}_\theta^p\cos\varphi\Big/\Big(\sqrt{3}\sin\varphi + \cos\varphi\Big) \tag{29}$$

Eq. (2) and Eq. (24) are also applicable to strain rates. Combining these equations gives

$$\partial\left(\dot{\varepsilon}_\theta^p\beta\right)/\partial\beta = -\partial\left(\dot{\varepsilon}_\theta^e\beta\right)/\partial\beta + \dot{\varepsilon}_r^p + \dot{\varepsilon}_r^e \tag{30}$$

Then, substituting Eq. (26) and Eq. (29) into Eq. (30) gives, with the use of Eq. (21),

$$\frac{E}{k}\left(\beta\frac{\partial\dot{\varepsilon}_\theta^p}{\partial\beta} + \sqrt{3}\dot{\varepsilon}_\theta^p\frac{\Phi_3}{\Phi_1}\right) = -\left[(1+\nu)\,\Phi_2\dot{\varphi} + \beta\left(\Phi_5\frac{\partial\dot{\varphi}}{\partial\beta} + \Phi_6\dot{\varphi}\frac{\partial\varphi}{\partial\beta}\right)\right] \tag{31}$$

where the derivative $\partial\varphi/\partial\beta$ follows from Eq.(18) and will be denoted by $D(\beta,\,\varphi)$

$$D(\beta,\,\varphi) = \partial\varphi/\partial\beta = \left[\beta^2\Omega + \Phi_3(\varphi)\right]/\left[\beta\Phi_1(\varphi)\right] \tag{32}$$

The time derivatives of functions involved in Eq. (31) may be written in the following form with Ω being a time-like variable

$$\begin{aligned}
\dot{\varepsilon}^p_\theta &= (\partial\varepsilon^p_\theta/\partial\Omega)\cdot(d\Omega/dt) = \xi^p_\theta\cdot(d\Omega/dt)\,,\\
\dot{\varphi} &= (\partial\varphi/\partial\Omega)\cdot(d\Omega/dt)\,,\\
\partial\dot{\varphi}/\partial\beta &= (\partial^2\varphi/\partial\Omega\partial\beta)\cdot(d\Omega/dt)
\end{aligned} \tag{33}$$

Analogously, it is possible to introduce the quantities

$$\begin{aligned}
\dot{\varepsilon}_\theta &= (\partial\varepsilon_\theta/d\Omega)\cdot(d\Omega/dt) = \xi_\theta\cdot(d\Omega/dt)\,,\\
\dot{\varepsilon}_r &= (\partial\varepsilon_r/d\Omega)\cdot(d\Omega/dt) = \xi_r\cdot(d\Omega/dt)\,,\\
\dot{\varepsilon}^p_r &= (\partial\varepsilon^p_r/d\Omega)\cdot(d\Omega/dt) = \xi^p_r\cdot(d\Omega/dt)\,,\\
\dot{\varepsilon}^e_r &= (\partial\varepsilon^e_r/d\Omega)\cdot(d\Omega/dt) = \xi^e_r\cdot(d\Omega/dt)\,,\\
\dot{\varepsilon}^e_\theta &= (\partial\varepsilon^e_\theta/d\Omega)\cdot(d\Omega/dt) = \xi^e_\theta\cdot(d\Omega/dt)\,,\\
\dot{\varepsilon}^E_r &= \left(\partial\varepsilon^E_r/d\Omega\right)\cdot(d\Omega/dt) = \xi^E_r\cdot(d\Omega/dt)\,,\\
\dot{\varepsilon}^E_\theta &= \left(\partial\varepsilon^E_\theta/d\Omega\right)\cdot(d\Omega/dt) = \xi^E_\theta\cdot(d\Omega/dt)
\end{aligned} \tag{34}$$

Then, Eq. (31) becomes

$$\begin{aligned}
&\beta\Phi_1\frac{\partial\xi^p_\theta}{\partial\beta} + \sqrt{3}\Phi_3\xi^p_\theta =\\
&\frac{k}{E}\left\{\frac{\partial\varphi}{\partial\Omega}\left[\frac{2}{\Phi_1}\left(\Phi_5 - \sqrt{3}\beta^2\Omega\right) - \Phi_3\Phi_6 - \Phi_1\Phi_2(1+\nu)\right] - \Phi_5\beta^2\right\}
\end{aligned} \tag{35}$$

The partial derivative $\partial\varphi/\partial\Omega$ can be found as a function of β from the

solution of the following equation obtained by differentiating Eq. (18) with respect to Ω

$$\beta\Phi_1^2\frac{\partial}{\partial\beta}\left(\frac{\partial\varphi}{\partial\Omega}\right)+\left[\Phi_4\left(\Omega\beta^2+\Phi_3\right)+\Phi_1\Phi_2\right]\frac{\partial\varphi}{\partial\Omega}-\beta^2\Phi_1=0 \tag{36}$$

It is now necessary to formulate the boundary conditions to Eqs. (35)-(36). Denote the value of φ at $\beta=q$ and $\beta=\gamma$ by φ_q and φ_γ, respectively. Obviously, φ_q and φ_γ are functions of Ω. Since the surface $\beta=q$ is motionless, the following equation is valid

$$(\partial\varphi/\partial\Omega)|_{\beta=q}=d\varphi_q/d\Omega \tag{37}$$

On the other hand, at the elastic-plastic boundary, $\beta=\gamma$,

$$\frac{\partial\varphi}{\partial\Omega}=\frac{d\varphi_\gamma}{d\Omega}-\frac{\partial\varphi}{\partial\beta}\frac{d\gamma}{d\Omega} \tag{38}$$

where $\partial\varphi/\partial\Omega$ and $\partial\varphi/\partial\beta$ should be taken at $\beta=\gamma$. The latter derivative is defined by Eq. (32). Therefore, Eq. (38) transforms to

$$\left.\frac{\partial\varphi}{\partial\Omega}\right|_{\beta=\gamma}=\frac{d\varphi_\gamma}{d\Omega}-D\left(\gamma,\ \varphi_\gamma\right)\frac{d\gamma}{d\Omega} \tag{39}$$

Differentiating Eq. (22) with respect to Ω gives the following relation between $d\varphi_\gamma/d\Omega$ and $d\gamma/d\Omega$

$$\frac{d\gamma}{d\Omega}=\frac{4\left[\gamma^2\Phi_2\left(\varphi_\gamma\right)+\sqrt{3}\Phi_3\left(\varphi_\gamma\right)\right]d\varphi_\gamma/d\Omega-\left[\gamma^4\left(1-\nu\right)+2\gamma^2\left(1+\nu\right)-3-\nu\right]}{4\gamma\left[\Omega\gamma^2\left(1-\nu\right)+\Omega\left(1+\nu\right)+2\Phi_3\left(\varphi_\gamma\right)\right]} \tag{40}$$

Substituting Eq. (40) into Eq. (39) yields

$$\left.\frac{\partial\varphi}{\partial\Omega}\right|_{\beta=\gamma}=\left[1-\frac{D\left(\gamma,\ \varphi_\gamma\right)\left[\gamma^2\Phi_2\left(\varphi_\gamma\right)+\sqrt{3}\Phi_3\left(\varphi_\gamma\right)\right]}{\gamma\left[\Omega\gamma^2\left(1-\nu\right)+\Omega\left(1+\nu\right)+2\Phi_3\left(\varphi_\gamma\right)\right]}\right]\frac{d\varphi_\gamma}{d\Omega}+$$
$$\frac{D\left(\gamma,\ \varphi_\gamma\right)\left[\gamma^4\left(1-\nu\right)+2\gamma^2\left(1+\nu\right)-3-\nu\right]}{4\gamma\left[\Omega\gamma^2\left(1-\nu\right)+\Omega\left(1+\nu\right)+2\Phi_3\left(\varphi_\gamma\right)\right]} \tag{41}$$

Equation (36) should satisfy both Eq. (37) and Eq. (41).

The boundary condition (8) is equivalent to

$$[\xi_\theta] = 0 \quad at \quad \beta = \gamma \tag{42}$$

Since $\xi_\theta = \xi_\theta^E$ on the elastic side of elastic-plastic boundary and $\xi_\theta = \xi_\theta^e + \xi_\theta^p$ on its plastic side, Eq. (42) transforms to

$$\xi_\theta^p = \xi_\theta^E - \xi_\theta^e \quad at \quad \beta = \gamma \tag{43}$$

The value of ξ_θ^e at $\beta = \gamma$ is defined by Eq. $(26)^2$, with the use of Eqs. (33)-(34). Excluding here $(\partial\varphi/\partial\Omega)|_{\beta=\gamma}$ by means of Eq. (39) gives

$$\xi_\theta^e = \frac{k}{E}\left(\frac{d\varphi_\gamma}{d\Omega} - D\left(\gamma,\, \varphi_\gamma\right)\frac{d\gamma}{d\Omega}\right)\Phi_5\left(\varphi_\gamma\right) \tag{44}$$

where γ is defined by Eq. (22) and $d\gamma/d\Omega$ by Eq. (40). The value of ξ_θ^E can be found by replacing A in Eq. $(13)^2$ by means of Eq. (23) and differentiating the resulting equation with respect to Ω

$$\begin{aligned} \xi_\theta^E \;=\; & -\frac{k}{4E\gamma\left(1+\gamma^2\right)^2}\left\{G_1\left(\gamma,\, \varphi_\gamma\right)\frac{d\varphi_\gamma}{d\Omega} + G_2\left(\gamma,\, \varphi_\gamma\right)\frac{d\gamma}{d\Omega} + \right. \\ & \left. \nu\gamma\left(1-\gamma^4\right)\left[3+\nu+\gamma^2\left(1-\nu\right)\right]\right\} \end{aligned} \tag{45}$$

where

$$G_1\left(\gamma,\, \varphi_\gamma\right) = 8\gamma\left[\gamma^4\left(1-\nu\right) + 2\gamma^2 + 1 + \nu\right]\cos\varphi_\gamma,$$

$$\begin{aligned} G_2\left(\gamma,\, \varphi_\gamma\right) = {} & \gamma^6\Omega\left(3\nu^2 - 2\nu - 1\right) + \gamma^4\Omega\left(3\nu^2 - 8\nu - 3\right) - \\ & -\gamma^2\left[\Omega\left(7\nu^2 + 10\nu - 1\right) - 16\left(1-\nu\right)\sin\varphi_\gamma\right] + \\ & \left(1+\nu\right)\left[\Omega\left(3+\nu\right) + 16\sin\varphi_\gamma\right] \end{aligned}$$

Here and in Eq. (44), γ should be excluded by means of Eq. (22) and $d\gamma/d\Omega$ by means of Eq. (40). Hence, substituting Eqs. (44)-(45) into Eq. (43) determines the value of ξ_θ^p at $\beta = \gamma$ in terms of φ_γ and $d\varphi_\gamma/d\Omega$. This value will be denoted by $\xi_\theta^p|_{\beta=\gamma}$.

The boundary condition (7) is equivalent to $\xi_\theta^p = -\xi_\theta^e$ at $\beta = q$. The value of ξ_θ^e can be found from Eqs. (26)^2, (33)-(34). Then, with the use of Eq. (37),

$$\xi_\theta^p = -\frac{k}{E}\frac{d\varphi_q}{d\Omega}\Phi_5(\varphi_q) \quad at \quad \beta = q \tag{46}$$

4 Numerical solution

Consider the generic line $\Omega = \Omega_{(i)}$ in the plastic zone (Fig.2) and assume that φ_q and $d\varphi_q/d\Omega$ at $\Omega = \Omega_{(i-1)}$ are known. The derivative $d\varphi_q/d\Omega$ within the interval $\Omega_{(i-1)} \le \Omega \le \Omega_{(i)}$ can be approximated as

$$\left.\frac{d\varphi_q}{d\Omega}\right|_{i-1,\,i} \approx \frac{1}{2}\left(\left.\frac{d\varphi_q}{d\Omega}\right|_{i-1} + \left.\frac{d\varphi_q}{d\Omega}\right|_{i}\right) \tag{47}$$

On the other hand,

$$\left.\frac{d\varphi_q}{d\Omega}\right|_{i-1,\,i} \approx \frac{\varphi_q|_i - \varphi_q|_{i-1}}{\Delta\Omega} \tag{48}$$

where $\Delta\Omega$ is the step in Ω, a small prescribed value. Combining Eqs. (47)-(48) gives

$$\left.\frac{d\varphi_q}{d\Omega}\right|_{i} = \frac{2\left(\varphi_q|_i - \varphi_q|_{i-1}\right)}{\Delta\Omega} - \left.\frac{d\varphi_q}{d\Omega}\right|_{i-1} \tag{49}$$

Consider point e (Fig.2) where $\varphi_\gamma = \varphi_q = \varphi_e$, $\Omega = \Omega_e = \Omega_{(0)}$ and $\gamma = q$. The values of φ_e and Ω_e are known due to Eq. (16) and Eq. (19). Combining Eq. (37) and Eq. (39) at this point it is possible to arrive at

$$\frac{d\varphi_q}{d\Omega} = \frac{d\varphi_\gamma}{d\Omega} - D(q,\ \varphi_e)\frac{d\gamma}{d\Omega} \tag{50}$$

The boundary condition (7) requires that $\xi_\theta^E = 0$ at point $e$where $\xi_\theta^E$is defined by Eq. (45). Combining this condition with Eq. (40) leads to the system of two equations with respect to $d\varphi_\gamma/d\Omega$ and $d\gamma/d\Omega$ at $\Omega = \Omega_e = \Omega_{(0)}$, $\varphi = \varphi_c$, $\gamma = q$. Substituting these derivatives into Eq. (50) gives the value of $d\varphi_q/d\Omega$ at $\Omega = \Omega_{(0)}$. Taking into account this value and following

the procedure outlined by Eq. (49), it is possible to find the derivative $d\varphi_q/d\Omega$ at $\Omega = \Omega_{(1)}$, let's denote it by $(d\varphi_q/d\Omega)|_1$, in terms of $\varphi_q|_1$. It is now necessary to solve Eqs. (18), (35)-(36) numerically at $\Omega = \Omega_{(1)}$. The boundary conditions for Eq. (18) and Eq. (36) are $\varphi = \varphi_q|_1$ and Eq. (37), respectively, where $d\varphi_q/d\Omega = (d\varphi_q/d\Omega)|_1$. The solution to these equations, with the use of Eqs. (22) and (41), determines, respectively, $\varphi_\gamma|_1$ and $(d\varphi_\gamma/d\Omega)|_1$. Therefore, $\xi_\theta^p|_{\beta=\gamma}$ at $\Omega = \Omega_{(1)}$ is found in terms of $\varphi_q|_1$. The value of $\xi_\theta^p|_{\beta=\gamma}$ may serve as a boundary condition to Eq. (35). However, the solution to Eq. (35) should also satisfy Eq. (46) which ultimately defines $\Delta\Omega$, and consequently $\varphi_q|_1$. Since the derivative $(d\varphi_q/d\Omega)|_1$ is now known, the procedure of finding distributions of φ, ξ_θ^p and other functions along β at $\Omega = \Omega_{(2)}$ can be repeated for $\Omega = \Omega_{(2)}$ and, then, for all other values $\Omega = \Omega_{(i)}$ at $i > 2$ as long as φ_q satisfies Eq. (20).

The derivative of radial displacement with respect to Ω is determined by

$$\partial u/\partial\Omega = \beta\,(\xi_\theta^p + \xi_\theta^e) \tag{51}$$

The distribution of the radial displacement is obtained by numerical integration in Eq. (51) after the distribution of ξ_θ^p and ξ_θ^e has been found in the entire interval of Ω. The boundary condition to (51) follows from (12) at $\beta = \gamma$.

5 Numerical examples and conclusions

The theory presented is illustrated by some numerical examples. The following material properties have been used in all calculations: $\nu = 0.3$, $E = 200 \times 10^3 MPa$, and $k = 127 MPa$.

Figs 3 through 5 show, respectively, the variation of φ_q, its derivative $d\varphi_q/d\Omega$, and the ratio γ/q, with the non-dimensional angular velocity parameter at different values of q. It is seen that the difference between the maximum possible angular velocity parameter corresponding to $\Omega_{\max}$ and the angular velocity parameter corresponding to Ω_e is very small. Here $\Omega_{\max}$ can be considered as the non-dimensional limit angular velocity and is the value of Ω at $\varphi_q = -\pi/6$. The larger the shaft radius, the lower angular velocity is required to reach $_{\max}$. It is also seen that the gradient

of $d\varphi_q/d\Omega$ is extremely high in the vicinity of $\Omega_{\max}$. It may lead to difficulties in numerical solutions for more complicated geometries where the analytical treatment of the problem is impossible. Fig. 5 shows that the maximum possible thickness of the plastic zone is very small as compared to the shaft radius. This result is very different from that obtained by means of a deformation theory of plasticity [11-13].

The variation of ξ_θ^p with Ω/Ω_e at different β is illustrated in Fig. 6. It is interesting to mention here that the function $\xi_\theta^p(\Omega)$ at specific values of β reaches a minimum near $\Omega = \Omega_{\max}$ and, then, when $\Omega \to \Omega_{\max}$, its gradient is very high.

The radial and circumferential stress distributions along the radius at different values of the non-dimensional angular velocity parameter are shown in Figs 7 and 8, respectively. In the plastic zone, σ_r and σ_θ are almost linear functions of β and the gradient of σ_θ is very high. To show better this qualitative effect of σ_θ distributions, the variation of σ_θ with the radius at different values of the non-dimensional angular velocity parameter is illustrated in Fig.9 by using another scale. The increase in angular velocity leads to substantial rise in the circumferential stress in the plastic region but does not produce such an effect with regard to the radial stress. While σ_θ reaches substantially high values in the plastic region, σ_r accordingly adjusts itself so that the stress state remains on the yield locus. Such variation of σ_θ with the radius is quite different from that found by means of a deformation theory of plasticity [11-13]. Even though variable thickness disks of strain-hardening material have been considered in these works, the disk of a constant thickness with no strain hardening is obtained as a special case.

The variation of the total radial and circumferential strains with the non-dimensional radius at different values of the non-dimensional angular velocity parameter is shown in Figs 10 and 11, respectively, and their plastic portions in Figs 12 and 13, respectively. The total circumferential strain is positive (Fig. 11) and slightly depends on Ω. However, its plastic portion is negative everywhere in the plastic zone (Fig. 13) and significantly depends on Ω. On the other hand, the solution predicts that the plastic portion of the radial strain is positive everywhere in the plastic zone (Fig. 12), and the total radial strain becomes negative only at the edge of the disk (Fig. 10). The gradient of the radial strain is very high in the plastic zone (theoretically infinite when $\varphi_q = -\pi/6$). This results

in a high gradient of the axial strain, ε_z, and to intensive thinning in a narrow zone near $\beta = q$. The same effect (but opposite in terms of the sign) has been found in [16] in the case of expansion of a hole in a plate under plane stress conditions. The behavior of the radial displacement (Fig. 14) is similar to that of total circumferential strain (Fig. 11).

Effects similar to the aforementioned ones also occur in disks with hard inclusions subject to thermal loading [6]. In the case of anisotropic rotating disks these effects can be even more pronounced, though it depends on the orientation of the principal axes of anisotropy. An illustrative example of the influence of anisotropy on the size of the plastic zone is given in [17]. Even though, the solution found is for perfectly plastic material, it may be more practical than the solutions found in [9–14] for strain hardening materials. First, the present solution is based on a more advanced theory of plasticity. Second, for materials with a yield plateau the elastic perfectly/plastic model adopted is more appropriate at small strains than models with strain hardening used in [9–14]. Moreover, even if hardening starts from the very beginning, it is believed that its influence on the qualitative behaviour of the solution is not so significant (though this question requires further investigations) and the assumption of plane stress plays the most important role.

Of special interest is comparison of solutions based on Tresca and Mises yield criteria. Under different conditions, such comparisons have been made in [4, 12, 18, 19, 20]. It has been mentioned that the difference between the solutions depends on the boundary conditions chosen. The boundary conditions accepted in the present paper have also been considered in [19, 20] where, however, a deformation theory of plasticity of strain-hardening material has been adopted (in [19, 20], disks of variable thickness have been considered but the disk of a constant thickness with no strain hardening is obtained as a special case). The comparison made in this paper does not show a significant difference between the solutions based on Tresca and Mises yield criteria. On the other hand, none of these solutions shows the qualitative effects demonstrated in the present solution, for example, the existence of the maximum angular velocity beyond which no solution exists, whereas the existence of such a velocity (or another parameter in the case of non-rotating disks) has been demonstrated in other thin disk problems solved with the use of the theory of plastic flow [16, 21]. Another important effect of the application of

Tresca yield criterion is that no plastic solution exits for a rotating solid disk [22]. In other words, it means that no plastic zone develops. On the other hand, under different sets of conditions the solution based on Tresca criterion predicts a greater spread of plasticity at similar angular velocities, as compared with the solution based on Mises criterion [21]. Taking into account a great variety of results on comparison of the two types of solutions, it is important to find the exact solution for the problem under consideration based on Tresca yield criterion and compare it with the present solution. This will be the subject of further investigations.

Acknowledgment

N.Alexandrova gratefully acknowledges support of this work from the Portuguese Science and Technology Foundation, grant SFRH / BPD/ 6549/ 2001, and S.Alexandrov acknowledges support through grant NSH-4472.2006.1 (Russia).

References

[1] A.N. Eraslan, *Elastoplastic deformations of rotating parabolic solid disks using Tresca's yield criterion*, Europ. J. Mech. A. Solids, **22**, (2003), 861-874.

[2] G. Ma, H. Hao and Y. Miyamoto, *Limit angular velocity of rotating disc with unified yield criterion*, Int. J. Mech. Sci., **43**, (2001), 1137-1153.

[3] M. Ghorashi and M. Daneshpazhooh, *Limit analysis of variable thickness circular plates*, Comp. Struct., **79**, (2001), 461-468.

[4] N. Alexandrova and S. Alexandrov, *Elastic-plastic stress distribution in a rotating annular disk*, Mech. Based Design Struct. Machines, **32**, (2004), 1-15.

[5] M. Kleiber and P. Kowalczyk, *Sensitivity analysis in plane stress elasto-plasticity and elasto-viscoplasticity*, Comp. Meth. Appl. Mech. Engrg, **137**, (1996), 395-409.

[6] S. Alexandrov and N. Chikanova, *Elastic-plastic stress-strain state of a plate with a pressed-in inclusion in thermal field*, Mech. Solids, **35**(4), (2000), 125-132 [trans.from Russian].

[7] S. Alexandrov and N. Alexandrova, *Thermal effects on the development of plastic zones in thin axisymmetric plates*, J. Strain Analysis Engng Design, **36**, (2001),169-176.

[8] N. Alexandrova, S. Alexandrov and P.M.M. Vila Real, *Displacement field and strain distribution in a rotating annular disk*, Mech. Based Design of Struct. Machines, **32**, (2004), 441-457.

[9] L.H. You, S.Y. Long and J.J. Zhang, *Perturbation solution of rotating solid disks with nonlinear strain-hardening*, Mech. Res. Comm., **24**, (1997), 649-658.

[10] L.H. You, Y.Y. Tang, J.J. Zhang and C.Y. Zheng, *Numerical analysis of elastic-plastic rotating disks with arbitrary variable thickness and density*, Int. J. Solids Struct., **37**, (2000), 7809-7820.

[11] A.N. Eraslan and H. Argeso, *Limit angular velocities of variable thickness rotating disks*, Int. J. Solids Struct., **39**, (2002), 3109-3130.

[12] A.N. Eraslan, *Inelastic deformations of rotating variable thickness solid disks by Tresca and von Mises criteria*, Int. J. Comput. Engrg Sci., **3**, (2002), 89-101.

[13] A.N. Eraslan, *Von Mises yield criterion and nonlinearity hardening variable thickness rotating annular disks with rigid inclusion*, Mech. Res. Comm., **29**, (2002), 339-350.

[14] A.N. Eraslan, Y. Orcan and U. Guven, *Elastoplastic analysis of nonlinearly hardening variable thickness annular disks under external pressure*, Mech. Res. Comm., **32**, (2005), 306-315.

[15] A. Nadai, *Theory of Flow and Fracture of Solids*, MsGraw-Hill, London, 1950.

[16] R. Hill, *Mathematical Theory of Plasticity*, Oxford Univ. Press, London, 1950.

[17] N. Alexandrova and S. Alexandrov, *Elastic-plastic stress distribution in a plastically anisotropic rotating disk*, Trans. ASME: J.Appl.Mech., **71**, (2004), 427-429.

[18] D.W.A. Rees, *Elastic-plastic stresses in rotating discs by von Mises and Tresca*, Z. Angew. Math. Mech, 79, (1999), 281-288.

[19] A.N. Eraslan, *Elastic-plastic deformations of rotating variable thickness annular disks with free, pressurized and radially constraint boundary conditions*, Int. J. Mech. Sci., 45, (2003), 643-667.

[20] A.N. Eraslan, *Stress distributions in elastic-plastic rotating disks with elliptical thickness profiles using Tresca and von Mises criteria,* Z. Angew. Math. Mech., 85, (2005), 252-266.

[21] D.W.A. Rees, *Basic Engineering Plasticity*, Elsevier, Amsterdam, 2006.

[22] U. Gamer, *Tresca's yield condition and the rotating disk*, Trans. ASME J. Appl. Mech., 50, (1983), 676-678.

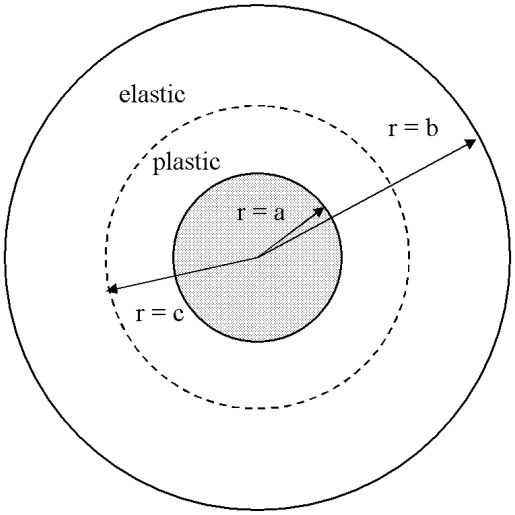

Figure 1: Rotating disk geometry.

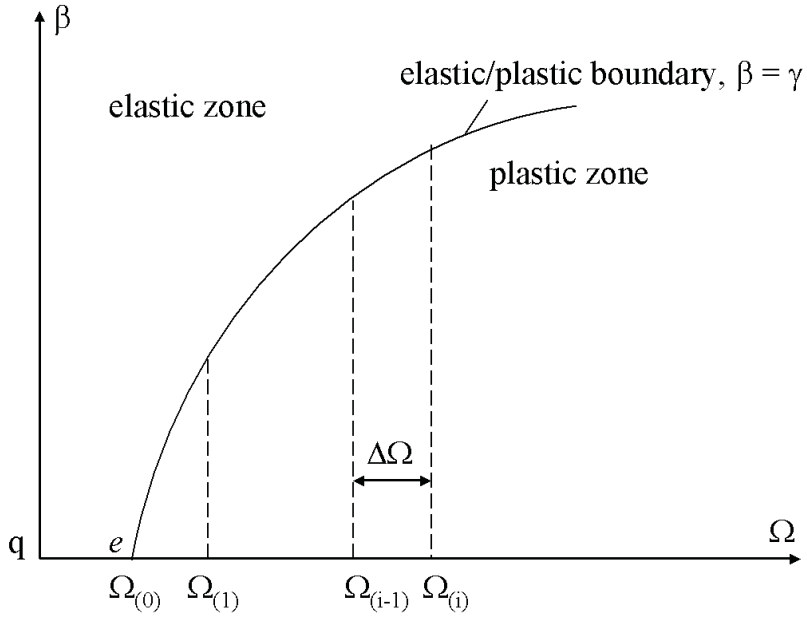

Figure 2: Illustration to the numerical procedure

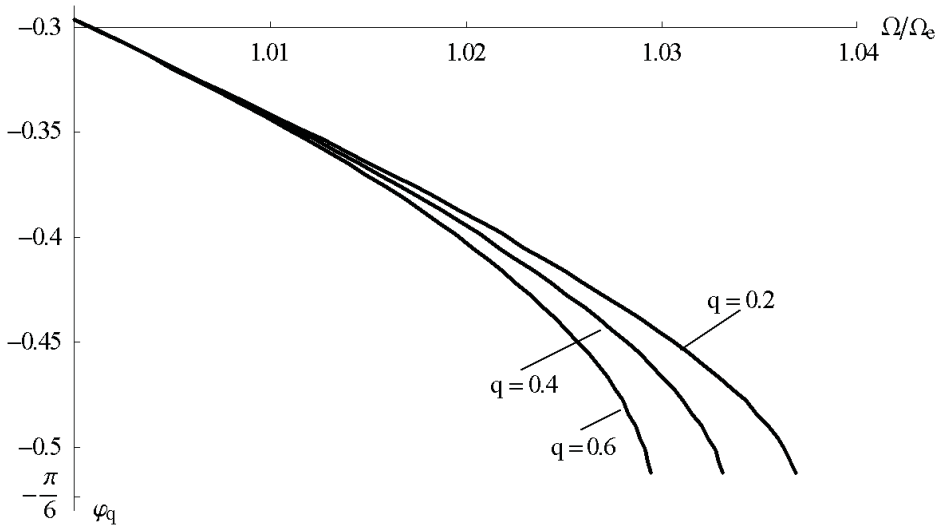

Figure 3: Variation of φ_q with Ω/Ω_e at different values of q.

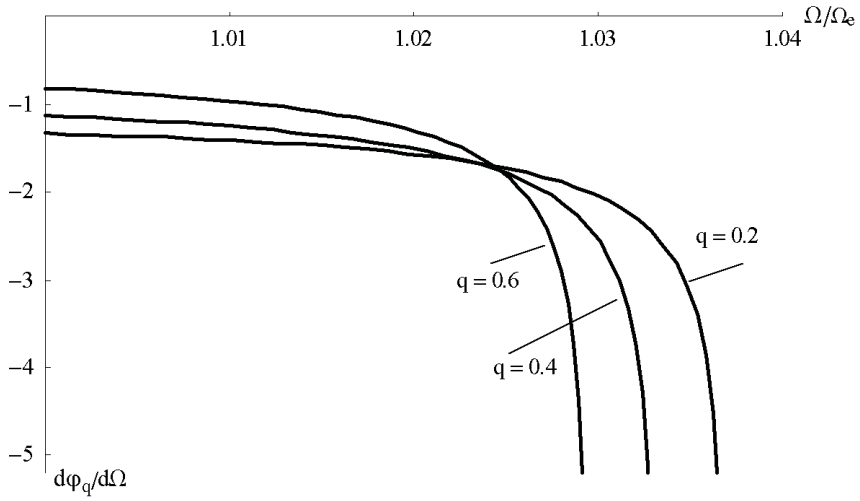

Figure 4: Variation of $d\varphi_q/d\Omega$ with Ω/Ω_e at different values of q.

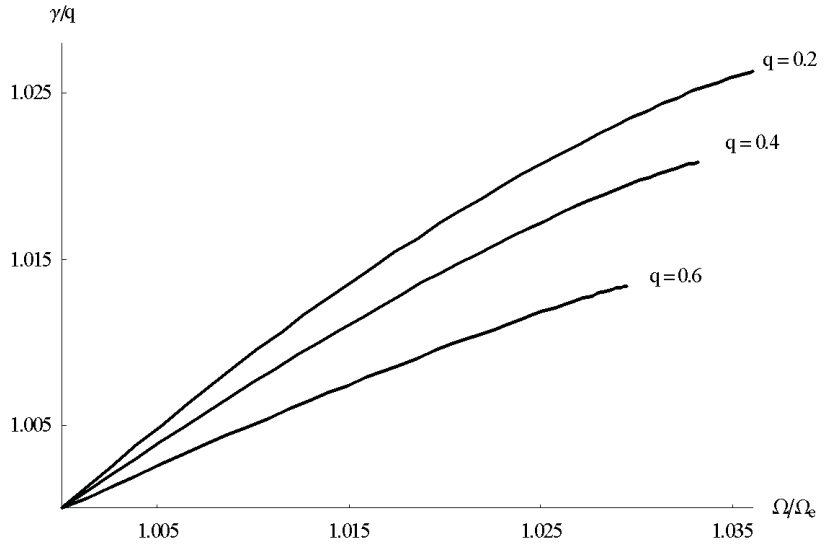

Figure 5: Variation of the ratio γ/q with Ω/Ω_e at different values of q.

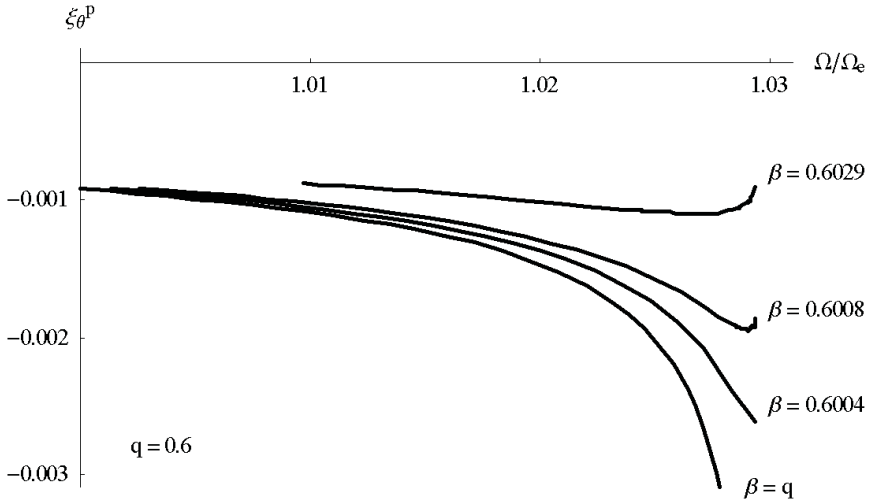

Figure 6: Variation of ξ_θ^p with Ω/Ω_e at different values of β.

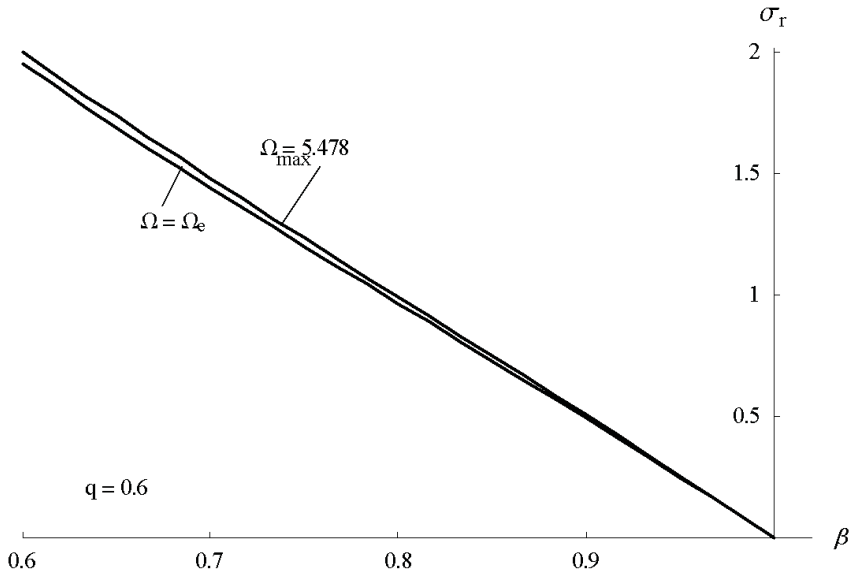

Figure 7: Radial stress distribution at $q = 0.6$ and different values of Ω.

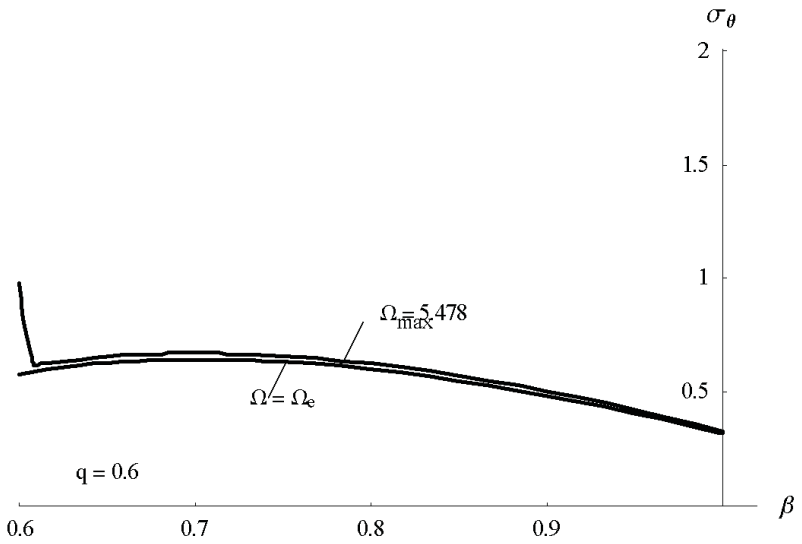

Figure 8: Hoop stress distribution at $q = 0.6$ and different values of Ω.

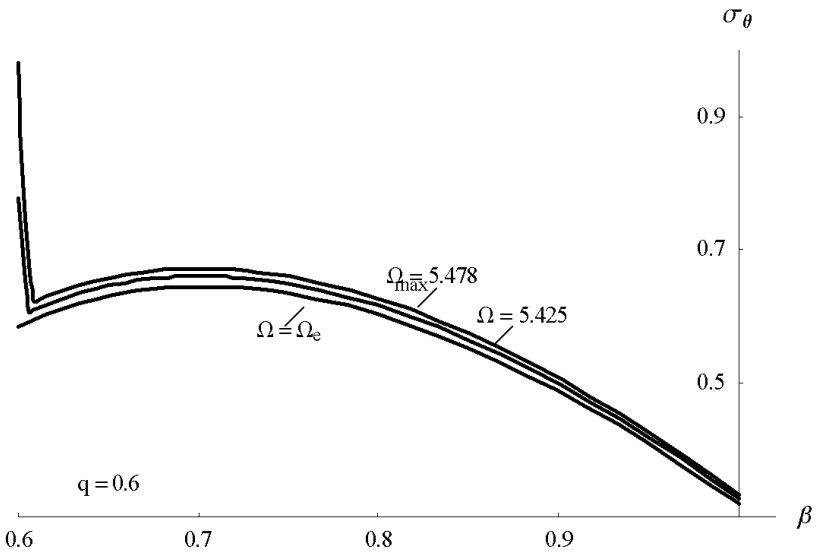

Figure 9: Hoop stress distribution at $q = 0.6$ and different values of Ω (different scale as compared to Fig.8).

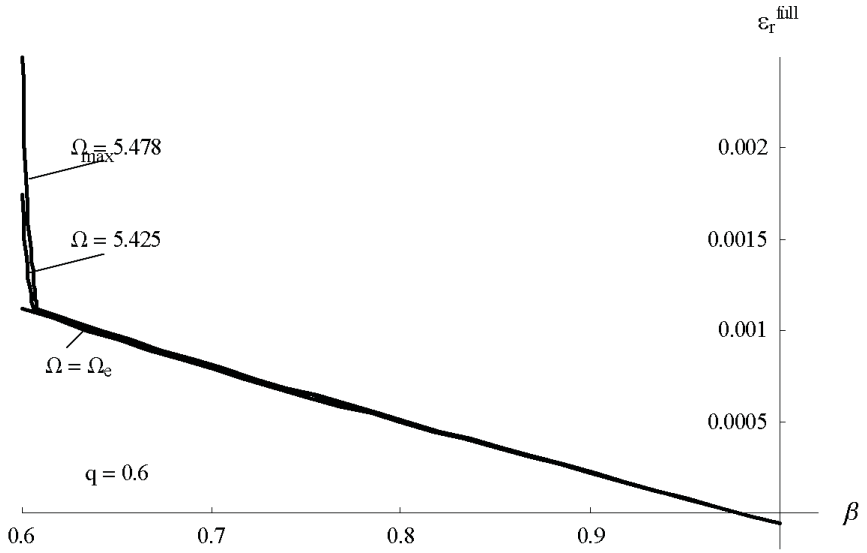

Figure 10: Full radial strain distribution at $q = 0.6$ and different values of Ω.

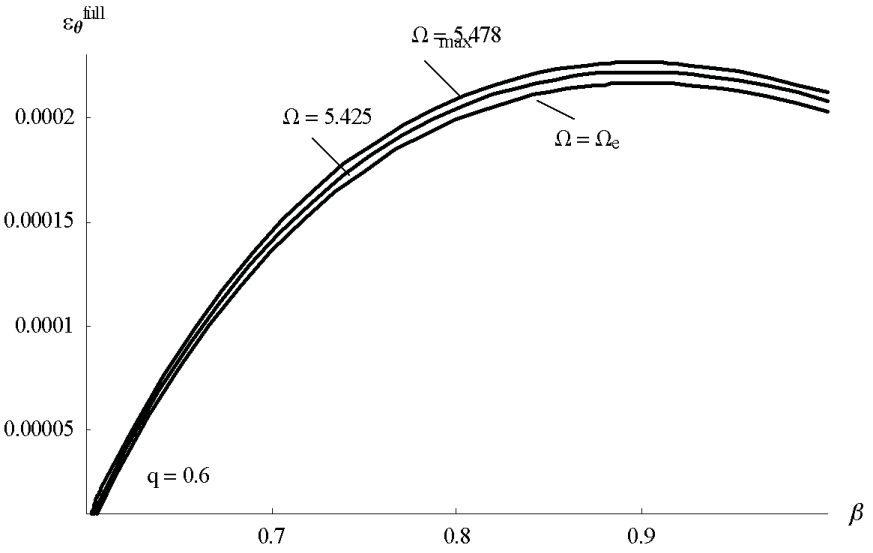

Figure 11: Full circumferential strain distribution at $q = 0.6$ and different values of Ω.

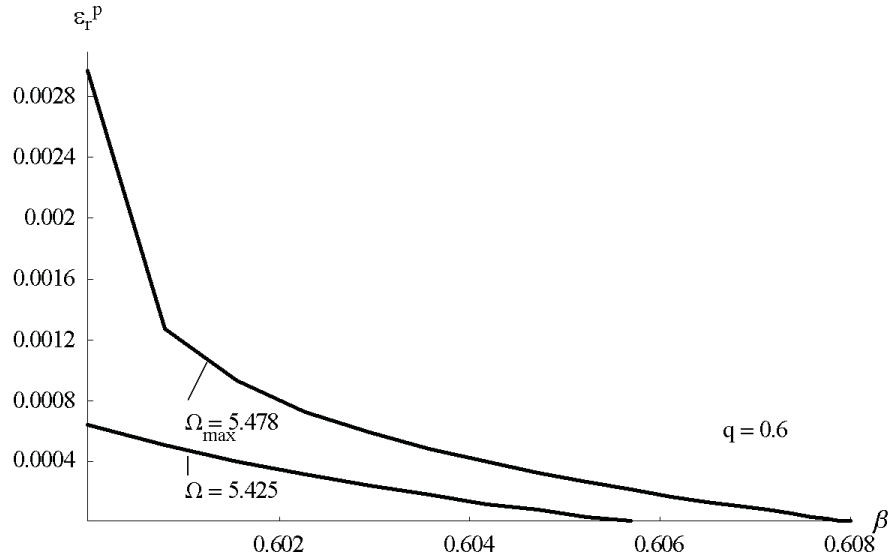

Figure 12: Plastic radial strain distribution at $q = 0.6$ and different values of Ω.

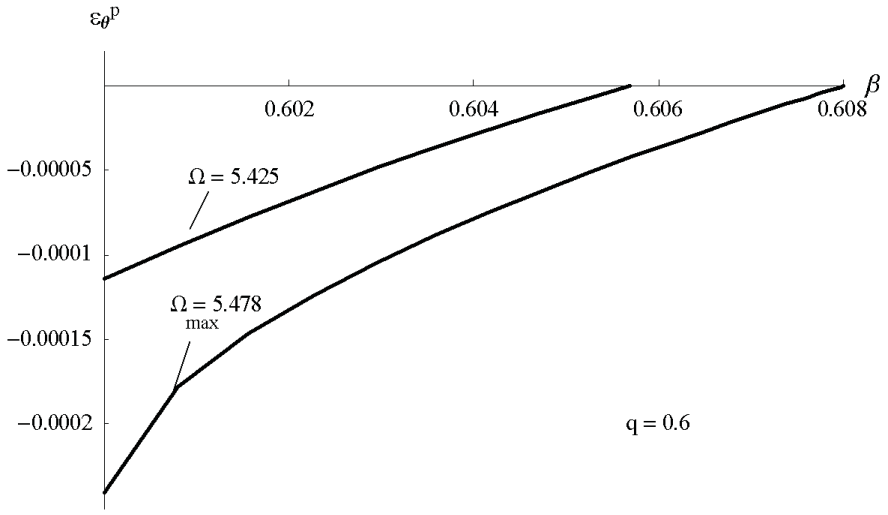

Figure 13: Plastic circumferential strain distribution at $q = 0.6$ and different values of Ω.

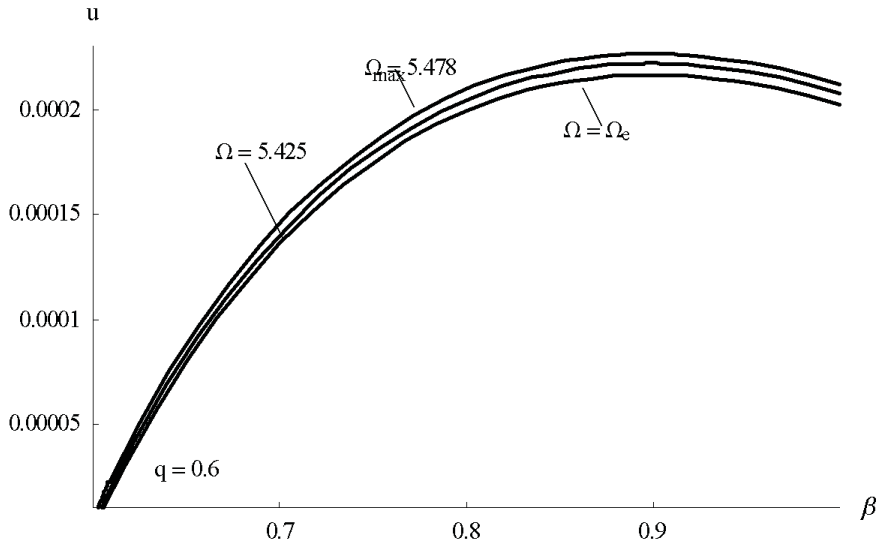

Figure 14: Radial displacement distribution at $q = 0.6$ and different values of Ω.

Submitted on September 2006.

Analiza napona i deformacije u obrtnom disku postavljenom na kruto vratilo

UDK 539.74

Proučava se ravansko naponsko stanje u elastično–idealno plastičnom izotropnom obrtnom disku sa centričnim otvorom. Analiza napona, deformacija i pomeranja unutar diska konstantne debljine i gustine zasniva se Mises-ovom pridruženom uslovu tečenja. Primećuje se da je plastična deformacija lokalizovana u blizini unutrašnjeg poluprečnika diska, tako da disk dovoljno velikog spoljnog poluprečnika nikada ne postaje potpuno plastičan. Poluanalitička metoda naponsko-deformacione analize je razvijena i ilustrovana nekim numeričkim primerima.